The effect of atmospheric sulfate reductions on diffuse radiation and photosynthesis in the United States during 1995 – 2013

G. Keppel-Aleks[1] and R. A. Washenfelder[2,3]

[1]Department of Climate and Space Sciences and Engineering, University of Michigan, Ann Arbor, MI, USA

[2]Cooperative Institute for Research in Environmental Sciences, University of Colorado, Boulder, CO, USA

[3]Chemical Sciences Division, Earth System Research Laboratory, National Oceanic and Atmospheric Administration, Boulder, CO, USA

Correspondence to: G. Keppel-Aleks (gkeppela@umich.edu)

Running title: Effect of SO_2 reductions on photosynthesis

Index terms: 0305 (Aerosols and particles), 0365 (Troposphere: composition and chemistry), 0360 (Radiation: transmission and scattering), 0345 (Pollution: urban and regional)

Keywords: Atmospheric aerosol, sulfate, optical properties, sulfur dioxide, photosynthesis, gross primary productivity, carbon sink

Key Points:

1. Aerosol optical depth has decreased due to reduced sulfur dioxide emissions.

This is the author manuscript accepted for publication and has undergone full peer review but has not been through the copyediting, typesetting, pagination and proofreading process, which may lead to differences between this version and the Version of Record. Please cite this article as doi: 10.1002/2016GL070052

2. Reduced diffuse radiation decreased cumulative gross primary productivity by 0.5 Pg C during 1995-2013.

3. CESM trends agree with upscaled flux tower results within 20%.

Abstract

Aerosol optical depth (AOD) has been shown to influence the global carbon sink by increasing the fraction of diffuse light, which increases photosynthesis over a greater fraction of the vegetated canopy. Between 1995 and 2013, U.S. SO_2 emissions declined by over 70%, coinciding with observed AOD reductions of 3.0 ± 0.6% y^{-1} over the eastern U.S. In the Community Earth System Model (CESM), these trends cause diffuse light to decrease regionally by almost 0.6% y^{-1}, leading to declines in gross primary production (GPP) of 0.07% y^{-1}. Integrated over the analysis period and domain, this represents 0.5 PgC of omitted GPP. A separate upscaling calculation that used published relationships between GPP and diffuse light agreed with the CESM model results within 20%.   The agreement between simulated and data-constrained upscaling results strongly suggests that anthropogenic sulfate trends have a small impact on carbon uptake in temperate forests due to scattered light.

1. Introduction

Terrestrial ecosystems affect climate by regulating fluxes of energy, water, and carbon. Currently, global ecosystems are a sink for anthropogenic CO_2 because gross primary productivity (GPP; the rate of photosynthesis) exceeds ecosystem respiration when integrated over an annual cycle. In order to quantify and predict the magnitude of the terrestrial carbon sink, it is necessary to understand the complex factors that affect GPP. On a global scale, temperature [*Cox et al.*, 2013; *Wang et al.*, 2013], growing season length [*Piao et al.*, 2007], atmospheric CO_2 concentrations [*Schimel et al.*, 2015; *Zhu et al.*, 2016], and water balance [*Gatti et al.*, 2014; *Nemani et al.*, 2002] all play important roles in controlling GPP variability.

Natural and anthropogenic aerosols may also affect the terrestrial carbon sink by scattering photosynthetically active radiation (PAR) to increase diffuse light and decrease direct light at the surface [*Mahowald*, 2011]. Diffuse light illuminates a greater fraction of the canopy, which increases light use efficiency and terrestrial carbon uptake [e.g. *Alton et al.*, 2007; *Dengel and Grace*, 2010; *Oliphant et al.*, 2011]. A number of observational studies have found positive correlations between diffuse radiation and photosynthesis [see references in *Kanniah et al.*, 2012]. Modeling studies have similarly suggested that this effect may be a significant driver of the global terrestrial carbon sink. For example, Mercado et al. [2009] concluded that diffuse light increased the strength of the land sink by one-quarter from 1960 to 1999 and Chen and Zhuang [2014] reported that present-day aerosol is responsible globally for 5 Pg C y^{-1} of GPP and 4 Pg C

y^{-1} of net ecosystem production (which exceeds the present-day land sink of ~3 Pg C y^{-1}) when compared to an aerosol-free control run.

The links among aerosol, scattered light, and photosynthesis indicate that changes in aerosol abundance can affect the magnitude of the land carbon sink. Anthropogenic primary and secondary aerosol make a large contribution to global aerosol mass [IPCC, 2013]. One of the major sources of anthropogenic aerosol is sulfur dioxide (SO_2) from coal-fired power plants and industrial processes, which is oxidized in the atmosphere to form sulfate (SO_4^{2-}) aerosol. As a result of the 1990 Clean Air Act Amendments in the United States, SO_2 emissions decreased 60% [*Hand et al.*, 2012], causing rapid changes in aerosol mass. For example, from 2001-2013 in the southeastern U.S., sulfate aerosol mass at surface sites decreased by 4.5(±0.9)% y^{-1} and aerosol optical depth (AOD) at 555 nm decreased by 3.5% y^{-1} [*Attwood et al.*, 2014]. As aerosol extinction decreases, both total radiation and the fraction of direct solar radiation at the surface increase [*Goldstein et al.*, 2009; *Ramanathan and Feng*, 2009], with potential effects on photosynthesis.

In this study, we examine the effect of decreasing SO_2 emissions on GPP within the eastern United States. We focus on the eastern U.S. because 1) rapid decreases in SO_2 emissions over the past two decades create an opportunity to examine the effects of reduced SO_4 mass and aerosol optical depth; 2) SO_2 emissions in the United States have been well quantified; 3) carbon fluxes within temperate ecosystems in the eastern United States have been well observed. We use accurate SO_2 emission data for 1995-2013 in the Community Earth System Model (CESM) to determine trends in AOD, surface radiation, and photosynthesis. We evaluate modeled AOD against satellite data, and compare the modeled photosynthetic response to an upscaled calculation constrained by published relationships between diffuse radiation and photosynthesis. By comparing simulations with a mechanistic land model and an empirically constrained upscaling, we show that even large reductions in aerosol precursor emissions have only modest impacts on regional GPP.

2. Methods

2.1 Approach 1: Community Earth System Model (CESM) determination of GPP

We simulated the impact of decreases in SO_2 emissions from the United States on aerosol optical depth, solar radiation, and terrestrial carbon exchange using the CESM atmosphere and land models.

2.1.1 Sulfur dioxide emissions inventory

We compiled an SO_2 emissions inventory for the United States based on Environmental Protection Agency (EPA) data from 1995-2013. The EPA requires the use of Continuous Emission Monitoring Systems (CEMS) to measure hourly emissions of SO_2 and NO_x for power plants and industrial sources regulated under the Acid Rain Program. This includes every unit that generates more than 25 MW of power and new units that generate less than 25 MW of power using fuel with sulfur content greater than 0.05% by weight [*Burns et al.*, 2011]. The

CEMS data has been validated with 38 aircraft transects downwind of Texas power plants during 2000 and 2006, which showed an average agreement of -0.7% ± 12.1% for SO_2/CO_2 ratios and an absolute accuracy of ~6% for CEMS SO_2 data [*Peischl et al.*, 2010]. We assigned the CEMS SO_2 sources to a 1° latitude × 1° longitude grid by month and year for 1995–2013 (Fig. 1a, b). CEMS monitoring accounted for 66-80% of U.S. SO_2 sources in the categories of "stationary fuel combustion" and "industrial and other processes" during 1995–2013 [US 2015], and the data was scaled to account for the unmonitored sources in these two categories, with the assumption that their geographical distribution is the same. We used the standard SO_2 emissions inventory for year 2000 for all sources outside the U.S., as well as for mobile sources, wildfires, agricultural burning, volcanoes, and domestic emissions within the U.S.[*Lamarque et al.*, 2010]. Chemical emissions of other species, including NO_x, were unchanged from the standard year 2000 model input [*Lamarque et al.*, 2010].

2.1.2 Chemistry, aerosol, and land models

We simulated the effect of SO_2 emission reductions on photosynthesis using a two-step process. First, we used the Community Atmosphere Model (CAM4.0) [*Neale et al.*, 2013] to simulate changes in diffuse and direct light as a consequence of SO_2 emissions reductions. Second, we used these radiation fields as input conditions to the Community Land Model (CLM4.5) [*Lawrence et al.*, 2012; *Lawrence et al.*, 2011] to simulate their impacts on land carbon uptake.

CAM4.0 was run at a horizontal resolution of $1.9^{\circ} \times 2.5^{\circ}$ using a finite volume dynamical core with 26 vertical levels. Ocean boundary conditions for this run were provided from a merged product that combines Hadley Centre sea ice and surface temperature data with higher resolution NOAA optimum interpolation analysis [*Hurrell et al.*, 2008]. Within CAM4.0, we used the Bulk Aerosol Model (BAM) to calculate gas- and aqueous-phase oxidation of SO_2 to sulfate and its contribution to aerosol mass [*Lamarque et al.*, 2012]. BAM efficiently computes the total mass of aerosol using an assumed lognormal size distribution. The optical properties of sulfate aerosol are computed in 14 shortwave bands (from 0.2-12.2 μm) using the Rapid Radiative Transfer Model (RRTMG) [*Mlawer et al.*, 1997]. RRTMG distinguishes between direct and diffuse solar radiation by parameterizing the scattering phase function using the Henyey-Greenstein approximation. These optical properties influence diffuse and direct radiation at visible (0.2-0.7 μm) and near-infrared (> 0.7 μm) wavelengths. To isolate the impact of SO_2 emissions reductions, other precursor emissions and greenhouse gas mole fractions were fixed at their year 2000 values. We ran the model for 19 years (1995-2013) and archived four radiation values (direct and diffuse radiation at visible and near-infrared wavelengths) at hourly resolution. We also archived AOD values for the 442-625 nm wavelength band.

The direct and diffuse visible and near-infrared radiation values from a single ensemble member were subsequently used as boundary conditions within CLM4.5 with reanalysis meteorology derived from Hadley Centre Climate Research Unit observations and National

Centers for Environmental Prediction (CRUNCEP) reanalysis data. We did not run a coupled land-atmosphere simulation due to coupling problems between CAM4 and CLM4.5 that have since been resolved in CAM5 (D. Lawrence, personal communication), but our approach provides realistic boundary conditions to the land model. We used annually repeating meteorological data to isolate the impact of diffuse light from interannual climate variability. CLM4.5 simulates biogeophysical interactions between the land surface and the atmosphere, including sensible and latent heat fluxes [*Lawrence et al.*, 2011]. Photosynthesis is simulated within CLM4.5 using a modified Ball-Berry model to relate stomatal conductance to net assimilation [*Lawrence et al.*, 2011]. Compared to prior versions, CLM4.5 better represents light use by sunlit and shaded leaves [*Bonan et al.*, 2011], and the maximum rate of carboxylation, $V_{c,max}$, is calculated separately for sunlit and shaded leaves since nitrogen allocation decreases with depth in the canopy. For our simulations, leaf area index in CLM4.5 was fixed according to satellite-derived phenology.

We spun-up CLM4.5 with the CRUNCEP temperature, precipitation, wind data, and year 1995 CAM4.0 diffuse and direct radiation until photosynthesis achieved steady state after approximately 200 years. We then used the archived radiation fields from CAM4.0/BAM to simulate the effect of decreasing diffuse fraction on monthly mean photosynthesis in CLM4.5 over 19 years. We assessed correlations between growing season (June, July, August; JJA) photosynthesis and radiation fields, but also calculated the annually integrated gross carbon uptake for our analysis. We calculated absolute trends in the data using ordinary least squares regression, and calculated relative trends (% y^{-1}) using ordinary least squares regression for the natural log of the variable.

2.2 Approach 2: Flux tower upscaling to determine GPP

Given the large range of model predictions for GPP-diffuse light correlations, we evaluated the accuracy of CESM GPP trends against an upscaling calculation constrained by eddy covariance flux observations. We used published relationships between radiation and GPP for different ecosystem types [*Cheng et al.*, 2015], and matched these to 17 land cover types determined from satellite observations (Table S1). Finally, we used direct and diffuse visible radiation from CAM4.0/BAM to calculate trends in photosynthesis during 1995-2013. This approach allowed us to make a simple calculation of the trend in photosynthesis, independent of the biogeophysics represented in the CLM4.5 model.

2.2.1 Land cover and radiation

Land cover type was taken from the Moderate Resolution Imaging Spectroradiometer (MODIS) L3 annual data (MCD12C1) with 0.05° resolution [*Friedl et al.*, 2010]. We used the International Geosphere-Biosphere Programme (IGBP) classification scheme, which includes 11 natural vegetation classes, three developed and mosaicked land classes, and three non-vegetated land classes [*Loveland and Belward*, 1997]. We neglected land cover changes in the U.S. over the study period, and used the 2001 land cover assignments for all years.

Direct and diffuse visible radiation were taken from CAM4.0/BAM, as described in Section 2.1.2. We scaled CESM visible radiation (0.2-0.7 μm) by 0.94 to match PAR (typically defined as 0.4-0.7 μm), based on observed ratios [*Gueymard*, 1989; *Papaioannou et al.*, 1993].

2.2.2 Published relationships between GPP, direct, and diffuse radiation

Cheng et al. [2015] used data from AmeriFlux towers in temperate forests and agricultural sites to calculate site-specific relationships between GPP, PAR_{direct} and $PAR_{diffuse}$. We represented GPP as:

$$GPP = \frac{\alpha\gamma PAR_{direct}}{\gamma + \alpha PAR_{direct}} + \beta_1 PAR_{diffuse} \quad (1)$$

where α is the canopy quantum efficiency, γ is the canopy photosynthetic potential, and β_1 is the slope of the relationship between photosynthesis and diffuse light, accounting for confounding impacts of direct light, air temperature, and vapor pressure deficit. We use the reported parameters for α, β_1, and γ from *Cheng et al.* [2015] averaged for solar zenith angles less than 60°, but neglected the effects of vapor pressure deficit and air temperature. We matched the four measurement locations (shown as open green circles in Fig. 3) from *Cheng et al.* [2015] to the 17 land cover types from the IGBP classification scheme. Further information and α, β_1, and γ values given in Table S1 of the Supplementary Material.

2.2.3 Error estimation

The uncertainty in the flux tower upscaling was calculated analytically from Eq. (1) for each 1.9 × 2.5 deg grid cell. The variability in visible direct and diffuse radiation modeled by CESM were determined from three CAM4.0/BAM model repetitions with identical emissions but different patterns of climate variability during the 19-year runs due to the sensitivity of the atmosphere to initial conditions. Interannual climate variability affects the chemical conversion of SO_2 to sulfate aerosol, the transport of both SO_2 and sulfate from source regions, and the influence of AOD on diffuse and direct radiation because it is modulated by clouds. The average uncertainty in α, β_1, and γ values were estimated to be 16%, 16%, and 2%, respectively (pers. comm. with S. J. Cheng). The uncertainty in MODIS IGBP land cover classifications was neglected. The average calculated uncertainty in the flux tower upscaling for the eastern U.S. was 27%.

2.3 Other Datasets

2.3.1 Satellite measurement of aerosol optical depth for model evaluation

The trends and magnitude of AOD at 550 nm from the CAM4.0 model were validated using Multi-Angle Imaging Spectroradiometer (MISR) L3 data at 555 nm with 0.5 deg resolution [*Kahn et al.*, 2009] for summer periods (JJA) during 2001-2013. AOD trends in the eastern

United States during 2001-2013 [-0.003 to -0.015 y^{-1}; *Attwood et al.*, 2014] were much greater than the MISR uncertainty [±0.0003 y^{-1}; *Zhang and Reid*, 2010].

3. Results and discussion

3.1 Trends in sulfur dioxide and aerosol optical depth

EPA emissions data indicate that total SO_2 emissions for the continental United States declined by more than 70% between 1995 and 2013 (Fig. 1c), from 1.6×10^{10} kg y^{-1} in 1995 to 0.4×10^{10} kg y^{-1} in 2013. The largest absolute changes occurred in the eastern and southeastern U.S. (Fig. 1b), and can be attributed to emission regulations implemented under the 1990 Clean Air Act and its amendments [*Burns et al.*, 2011; *Hand et al.*, 2012] (Fig. 1c).

AOD likewise decreased over the eastern and southeastern U.S. during this time period. Both the MISR satellite and the CESM model simulated AOD decreases of several percent per year across the eastern US, and the largest decreases were geographically coincident with decreased SO_2 emissions (Fig. 2). During the period from 2001 to 2013, when both MISR and CESM data are available, MISR measured an average AOD trend of -3.0 ± 0.6% y^{-1} with a mean AOD of 0.19 over the eastern U.S. (yellow outlined area in Fig. 2a, b). For the same area and time period, the CESM model simulated an average AOD trend of -4.9 ± 0.3% y^{-1} with a mean AOD of 0.22, using an accurate SO_2 emissions inventory and other emissions held constant at their year 2000 values. In addition to decreasing aerosol SO_4 mass, the MISR measurements are influenced by smaller trends due to decreasing aerosol nitrate, elemental carbon, and organic carbon mass [*Hand et al.*, 2014], so we do not expect absolute agreement with the CESM model. However, the fact that CESM simulates both absolute values and trends in AOD that are similar to the MISR observations indicates that the CAM4.0/BAM model is able to accurately simulate aerosol extinction based on SO_2 emissions, and further suggests that CAM4.0 reasonably represents direct and diffuse radiation trends.

3.2 Trend in diffuse radiation and photosynthesis from CESM model

The CESM model simulates an absolute decline in diffuse radiation of 0.2-0.3W m^{-2} y^{-1} during JJA from 1995-2013 over the eastern U.S., equivalent to a relative trend of -0.6 ± 0.2% y^{-1} (Fig. 3a). Diffuse and direct radiation covary, and CESM simulates an increase in direct radiation of 0.3 ± 0.2% y^{-1} for the same time period, resulting in a total visible radiation increase of 0.1 ± 0.2% y^{-1}.

When these radiation values are input as boundary conditions to the Community Land Model (CLM4.5) with CRUNCEP reanalysis meteorology, the simulated trend is -0.11 ± 0.04% y^{-1} for JJA GPP and -0.07 ± 0.03% y^{-1} for annual GPP from 1995-2013 over the Eastern U.S. (Fig. 3b). The absolute decline was 4.5 ± 2.0 Tg C y^{-2}. Modeled GPP for a control simulation with diffuse and direct radiation fields fixed at their 1995 values does not show significant trends (Fig. S1). Over the 19 years of our study, these trends represent a cumulative reduction in gross carbon uptake of 1.1 ± 0.04% over the eastern U.S., which is equivalent to about 0.5 Pg C of omitted photosynthesis due to reductions in SO_2 emissions relative to the control.

Differences in the GPP trend across the eastern U.S. were tied primarily to the magnitude of change in diffuse light. Because atmospheric variables were prescribed from CRUNCEP reanalysis, vegetation temperature increased by only 0.003 K y^{-1} averaged over the eastern U.S., and trends at the grid cell level were not statistically significant at the 95% confidence level. Rather, the relative trend in photosynthesis was correlated with the magnitude of the diffuse light decrease. The southeastern U.S. (south of 40°N) saw both the largest trend in diffuse light and the largest relative trend in photosynthesis, about one-third greater than the relative trend north of 40°N (Fig. 3b, c). The grid cells with the largest trends contained plant functional types in equal proportion to the entire domain, suggesting that vegetation distributions did not drive the spatial variability. Multiple linear regression did not show statistically significant differences for the diffuse light efficiency for different plant functional types, nor did it yield robust results for separating the influence of direct and diffuse light.

3.3 Trend in photosynthesis from flux tower upscaling

Figure 4 shows temporal trends in AOD, diffuse radiation, and GPP from the CESM model for the eastern U.S., together with the trend in GPP determined from the flux tower upscaling. Photosynthesis decreased on average by -0.97 ± 0.19 gC m^{-2} y^{-1} over 19 years for the eastern U.S. (Fig 4a) when calculated using Eq. 1 with direct and diffuse visible radiation from

CESM. The trends are geographically consistent with those from the CESM model (Fig. 3b, d.). For the Eastern U.S., the trend predicted by CEMS is consistent with the flux tower upscaling within 9% (Table 1) while a scatter plot of the individual values shows consistency of 20% (Fig. 3e). Fig. 4b and c show model and flux tower upscaling results for the SEARCH site in Centreville, Alabama where large reductions in AOD have occurred and the UMBS field site from Cheng et al. [2015] where more modest reductions in AOD have occurred.

4. Discussion and Conclusions

The CESM model predicts that the reduction in SO_2 emissions associated with the Clean Air Act Amendments has led to a 4.9 ± 0.3% y^{-1} change in AOD and a 3.0 ± 0.6% y^{-1}decline in diffuse radiation over the eastern U.S. between 1995 and 2013. We confirmed that simulation of AOD within CESM is in good agreement with MISR data for accurate historical SO_2 emissions. The impact of these changes on photosynthesis rates is confirmed by a simple flux tower upscaling calculation, which finds a consistent change in GPP over the eastern U.S. during the same period. These results suggest that the 1990 Clean Air Act Amendments, while improving air quality, had a small adverse impact on the U.S. carbon sink attributed to changes in direct and diffuse radiation.

Our results suggest that over a 19 year period, only 0.5 Pg C of GPP was omitted over the eastern US despite significant changes in AOD and diffuse radiation. The small effect that we find in both CESM and the observationally constrained upscaling disagrees with recent results from *Strada and Unger* [2016], who report that anthropogenic aerosols enhance GPP by 5-8% annually over temperate ecosystems in eastern North America. Given that in our observationally constrained upscaling, the cumulative reduction in GPP was only 1%, their model result likely overestimates the influence of anthropogenic aerosol on GPP. Our results are more consistent with *Xia et al.* [2016], who used CLM4 to calculate that a ~3 W m^{-2} increase in diffuse light under a geoengineering scenario increases temperate forest photosynthesis by ~0.07 μmol C m^{-2} s^{-1}, which agrees within a factor of two with our sensitivities from both CESM using CLM4.5 and the flux tower upscaling. The disparate results from different models underscores the importance of simulating quantities that can be compared to available observations. While our study considers only the impacts on photosynthesis, not net ecosystem exchange, we expect that the overall decrease to the land carbon sink is smaller than 0.5 PgC integrated over 20 years due to respiration. Although this value only comprises the Eastern U.S., the small change to photosynthesis resulting from a large change in sulfate aerosol does not support a substantial role for diffuse light impacts from anthropogenic aerosol as a driver of the historical land carbon sink (e.g., [*Mercado et al.*, 2009]). Our results also suggest a minimal trade-off between future reductions in anthropogenic aerosol for improved air quality and their indirect impacts on the land carbon sink, at least in temperate ecosystems.

The decrease in SO_2 and NO_x ($NO + NO_2$) emissions due to the Clean Air Act Amendments are expected to have other impacts on carbon uptake that may enhance or offset the impacts of sulfate aerosol. Both SO_2 and NO_x contribute to acid deposition, which depletes nutrients such as calcium, magnesium, and potassium in the soil, and may contribute to tree mortality [*Driscoll et al.*, 2001]. Ozone is produced through photochemistry that requires NO_x, and its presence causes plant cellular damage through the degradation of stomata and reduced water use efficiency [*Holmes*, 2014; *Lombardozzi et al.*, 2015]. Decreased acid deposition and ozone concentration would both increase photosynthesis over the period from 1995-2013, counteracting the effect of reduced sulfate aerosol. Alternatively, decreased nitrogen deposition due to reduced NO_x emissions may decrease photosynthesis in nitrogen-limited ecosystems. This effect is likely small because eastern forests are only moderately sensitive to nitrogen additions [*Nadelhoffer et al.*, 1999], and chronic nitrogen additions may actually slow rates of carbon uptake [*Aber et al.*, 1989]. In contrast to our simulations, which were run with fixed climate, decreased AOD may lead to increased surface temperatures and reductions in photosynthesis. We designed our simulations to minimize this effect and to facilitate comparisons with the observational scale factors derived from *Cheng et al.* [2015]. Likewise, we have considered only the influence of sulfate aerosol on the aerosol direct effect and photosynthesis, independent from other factors which may have changed direct and diffuse radiation during the period from 1995-2013. Biogenic emissions that contribute to secondary organic aerosol may decrease as diffuse light decreases [*Strada and Unger*, 2016; *Wilton et al.*, 2011], although the magnitude is not well constrained and may be counteracted by covarying temperature increases [*Knohl and Baldocchi*, 2008]. Surface radiation data has shown increasing trends in both clear-sky total and diffuse shortwave radiation in the U.S., and this has been attributed to factors such as high-altitude cirrus or cloudiness [*Gan et al.*, 2014; *Long et al.*, 2009].

Uncertainty persists in the net impact anthropogenic activity has on ecosystem carbon uptake, and climate change predictions require accurate accounting of the radiative forcing of CO_2, as well as accurate accounting of numerous climate feedbacks that are driven by aerosol. Although we found that the effect of diffuse radiation on photosynthesis was small for the U.S., quantifying this interaction is an important step that should be considered for ecosystems globally. Future aerosol trends will likely be dominated by changes in anthropogenic emissions from China and other countries.

Acknowledgements

The research was supported in part by the Biogeochemistry – Climate Feedbacks Scientific Focus Area (SFA), which is sponsored by the Regional and Global Climate Modeling (RGCM) Program in the Climate and Environmental Sciences Division (CESD) of the Biological and Environmental Research Program in the U.S. Department of Energy Office of Science. We thank Greg Frost for advice about SO_2 emissions inventories. We thank Susan Cheng and Allison Steiner for helpful discussions on the flux tower data, and Mark Flanner for discussions about configuring CESM. Data are available from the authors upon request.

References

Aber, J. D., K. J. Nadelhoffer, P. Steudler, and J. M. Melillo (1989), Nitrogen Saturation in Northern Forest Ecosystems, *BioScience, 39*(6), 378-386, doi:10.2307/1311067.

Alton, P. B., P. R. North, and S. O. Los (2007), The impact of diffuse sunlight on canopy light-use efficiency, gross photosynthetic product and net ecosystem exchange in three forest biomes, *Global Change Biol.*, *13*(4), 776-787.

Attwood, A. R., et al. (2014), Trends in sulfate and organic aerosol mass in the Southeast U.S.: Impact on aerosol optical depth and radiative forcing, *Geophys. Res. Lett.*, *41*(21), 7701-7709.

Bonan, G. B., P. J. Lawrence, K. W. Oleson, S. Levis, M. Jung, M. Reichstein, D. M. Lawrence, and S. C. Swenson (2011), Improving canopy processes in the Community Land Model version 4 (CLM4) using global flux fields empirically inferred from FLUXNET data, *J. Geophys. Res.-Biogeo.*, *116*.

Burns, D. A., J. A. Lynch, B. J. Cosby, M. E. Fenn, and J. S. Baron (2011), National Acid Precipitation Assessment Program report to Congress 2011: An integrated assessment*Rep.*, 114 pp, National Science and Technology Council.

Chen, M., and Q. L. Zhuang (2014), Evaluating aerosol direct radiative effects on global terrestrial ecosystem carbon dynamics from 2003 to 2010, *Tellus B, 66*, doi:10.3402/tellusb.v3466.21808.

Cheng, S. J., G. Bohrer, A. L. Steiner, D. Y. Hollinger, A. Suyker, R. P. Phillips, and K. J. Nadelhoffer (2015), Variations in the influence of diffuse light on gross primary productivity in temperate ecosystems, *Agr. Forest Meteorol.*, *201*, 98-110.

Cox, P. M., D. Pearson, B. B. Booth, P. Friedlingstein, C. Huntingford, C. D. Jones, and C. M. Luke (2013), Sensitivity of tropical carbon to climate change constrained by carbon dioxide variability, *Nature*, *494*(7437), 341-344.

Dengel, S., and J. Grace (2010), Carbon dioxide exchange and canopy conductance of two coniferous forests under various sky conditions, *Oecologia*, *164*(3), 797-808.

Driscoll, C. T., G. B. Lawrence, A. J. Bulger, T. J. Butler, C. S. Cronan, C. Eagar, K. F. Lambert, G. E. Likens, J. L. Stoddard, and K. C. Weathers (2001), Acidic deposition in the northeastern United States: Sources and inputs, ecosystem effects, and management strategies, *BioScience*, *51*(3), 180-198.

Friedl, M. A., D. Sulla-Menashe, B. Tan, A. Schneider, N. Ramankutty, A. Sibley, and X. M. Huang (2010), MODIS collection 5 global land cover: Algorithm refinements and characterization of new datasets, *Remote Sens. Environ.*, *114*(1), 168-182.

Gan, C. M., J. Pleim, R. Mathur, C. Hogrefe, C. N. Long, J. Xing, S. Roselle, and C. Wei (2014), Assessment of the effect of air pollution controls on trends in shortwave radiation over the United States from 1995 through 2010 from multiple observation networks, *Atmos. Chem. Phys.*, *14*(3), 1701-1715.

Gatti, L. V., et al. (2014), Drought sensitivity of Amazonian carbon balance revealed by atmospheric measurements, *Nature*, *506*(7486), 76-80, doi:10.1038/nature12957.

Goldstein, A. H., C. D. Koven, C. L. Heald, and I. Y. Fung (2009), Biogenic carbon and anthropogenic pollutants combine to form a cooling haze over the southeastern United States, *P. Natl. Acad. Sci. USA*, *106*(22), 8835-8840.

Gueymard, C. (1989), A two-band model for the calculation of clear sky solar irradiance, illuminance, and photosynthetically active radiation at the earth's surface, *Solar Energy*, *43*(5), 253-265, doi:http://dx.doi.org/10.1016/0038-092X(89)90113-8.

Hand, J. L., B. A. Schichtel, W. C. Malm, S. Copeland, J. V. Molenar, N. Frank, and M. Pitchford (2014), Widespread reductions in haze across the United States from the early 1990s through 2011, *Atmos Environ*, *94*, 671-679.

Hand, J. L., B. A. Schichtel, W. C. Malm, and M. L. Pitchford (2012), Particulate sulfate ion concentration and SO_2 emission trends in the United States from the early 1990s through 2010, *Atmos. Chem Phys.*, *12*(21), 10353-10365.

Holmes, C. D. (2014), Air pollution and forest water use, *Nature*, *507*(7491), E1-E2, doi:10.1038/nature13113.

Hurrell, J. W., J. J. Hack, D. Shea, J. M. Caron, and J. Rosinski (2008), A New Sea Surface Temperature and Sea Ice Boundary Dataset for the Community Atmosphere Model, *J Climate*, *21*(19), 5145-5153, doi:10.1175/2008JCLI2292.1.

Kahn, R. A., D. L. Nelson, M. J. Garay, R. C. Levy, M. A. Bull, D. J. Diner, J. V. Martonchik, S. R. Paradise, E. G. Hansen, and L. A. Remer (2009), MISR aerosol product attributes and statistical comparisons with MODIS, *IEEE T. Geosci. Remote*, *47*(12), 4095-4114.

Kanniah, K. D., J. Beringer, P. North, and L. Hutley (2012), Control of atmospheric particles on diffuse radiation and terrestrial plant productivity: A review, *Prog. Phys. Geog.*, *36*(2), 209-237.

Knohl, A., and D. D. Baldocchi (2008), Effects of diffuse radiation on canopy gas exchange processes in a forest ecosystem, *Journal of Geophysical Research: Biogeosciences*, *113*(G2), n/a-n/a, doi:10.1029/2007JG000663.

Lamarque, J. F., et al. (2010), Historical (1850-2000) gridded anthropogenic and biomass burning emissions of reactive gases and aerosols: methodology and application, *Atmos. Chem. Phys.*, *10*(15), 7017-7039.

Lamarque, J. F., et al. (2012), CAM-chem: Description and evaluation of interactive atmospheric chemistry in the Community Earth System Model, *Geosci. Model Dev.*, *5*(2), 369-411.

Lawrence, D. M., K. W. Oleson, M. G. Flanner, C. G. Fletcher, P. J. Lawrence, S. Levis, S. C. Swenson, and G. B. Bonan (2012), The CCSM4 land simulation, 1850-2005: Assessment of surface climate and new capabilities, *J. Climate*, *25*(7), 2240-2260.

Lawrence, D. M., et al. (2011), Parameterization improvements and functional and structural advances in version 4 of the community land model, *J. Adv. Model. Earth Sy.*, *3*, 2011MS000045.

Lombardozzi, D., S. Levis, G. Bonan, P. G. Hess, and J. P. Sparks (2015), The influence of chronic ozone exposure on global carbon and water cycles, *J. Climate*, *28*(1), 292-305, doi:10.1175/JCLI-D-14-00223.1.

Long, C. N., E. G. Dutton, J. A. Augustine, W. Wiscombe, M. Wild, S. A. McFarlane, and C. J. Flynn (2009), Significant decadal brightening of downwelling shortwave in the continental United States, *J. Geophys. Res.*, *114*(D00D06), doi:10.1029/2008JD011263.

Loveland, T. R., and A. S. Belward (1997), The IGBP-DIS global 1 km land cover data set, DISCover: First results, *Int. J. Remote Sens.*, *18*(15), 3291-3295.

Mahowald, N. (2011), Aerosol indirect effect on biogeochemical cycles and climate, *Science*, *334*(6057), 794-796.

Mercado, L. M., N. Bellouin, S. Sitch, O. Boucher, C. Huntingford, M. Wild, and P. M. Cox (2009), Impact of changes in diffuse radiation on the global land carbon sink, *Nature*, *458*(7241), 1014-1017.

Mlawer, E. J., S. J. Taubman, P. D. Brown, M. J. Iacono, and S. A. Clough (1997), Radiative transfer for inhomogeneous atmospheres: RRTM, a validated correlated-k model for the longwave, *J. Geophys. Res.*, *102*(D14), 16663-16682.

Nadelhoffer, K. J., B. A. Emmett, P. Gundersen, O. J. Kjonaas, C. J. Koopmans, P. Schleppi, A. Tietema, and R. F. Wright (1999), Nitrogen deposition makes a minor contribution to carbon sequestration in temperate forests, *Nature*, *398*(6723), 145-148.

Neale, R. B., J. Richter, S. Park, P. H. Lauritzen, S. J. Vavrus, P. J. Rasch, and M. H. Zhang (2013), The mean climate of the Community Atmosphere Model (CAM4) in forced SST and fully coupled experiments, *J. Climate*, *26*(14), 5150-5168.

Nemani, R., M. White, P. Thornton, K. Nishida, S. Reddy, J. Jenkins, and S. Running (2002), Recent trends in hydrologic balance have enhanced the terrestrial carbon sink in the United States, *Geophys. Res. Lett.*, *29*(10), 106-101-106-104, doi:10.1029/2002GL014867.

Oliphant, A. J., D. Dragoni, B. Deng, C. S. B. Grimmond, H. P. Schmid, and S. L. Scott (2011), The role of sky conditions on gross primary production in a mixed deciduous forest, *Agr. Forest Meteorol.*, *151*(7), 781-791.

Papaioannou, G., N. Papanikolaou, and D. Retalis (1993), Relationships of photosynthetically active radiation and shortwave irradiance, *Theoretical and Applied Climatology*, *48*(1), 23-27, doi:10.1007/BF00864910.

Peischl, J., et al. (2010), A top-down analysis of emissions from selected Texas power plants during TexAQS 2000 and 2006, *J Geophys Res-Atmos*, *115*.

Piao, S., P. Friedlingstein, P. Ciais, N. Viovy, and J. Demarty (2007), Growing season extension and its impact on terrestrial carbon cycle in the Northern Hemisphere over the past 2 decades, *Global Biogeochem. Cy.*, *21*(3), GB3018, doi:10.1029/2006GB002888.

Ramanathan, V., and Y. Feng (2009), Air pollution, greenhouse gases and climate change: Global and regional perspectives, *Atmos. Environ.*, *43*(1), 37-50.

Schimel, D., B. B. Stephens, and J. B. Fisher (2015), Effect of increasing CO_2 on the terrestrial carbon cycle, *P. Natl. Acad. Sci. USA*, *112*(2), 436-441.

Strada, S., and N. Unger (2016), Potential sensitivity of photosynthesis and isoprene emission to direct radiative effects of atmospheric aerosol pollution, *Atmos. Chem. Phys.*, *16*(7), 4213-4234, doi:10.5194/acp-16-4213-2016.

Wang, W., P. Ciais, R. R. Nemani, J. G. Canadell, S. Piao, S. Sitch, M. A. White, H. Hashimoto, C. Milesi, and R. B. Myneni (2013), Variations in atmospheric CO_2 growth rates coupled with tropical temperature, *P. Natl. Acad. Sci. USA*, *110*(32), 13061-13066.

Wilton, D. J., C. N. Hewitt, and D. J. Beerling (2011), Simulated effects of changes in direct and diffuse radiation on canopy scale isoprene emissions from vegetation following volcanic eruptions, *Atmos. Chem. Phys.*, *11*(22), 11723-11731, doi:10.5194/acp-11-11723-2011.

Xia, L., A. Robock, S. Tilmes, and R. R. Neely Iii (2016), Stratospheric sulfate geoengineering could enhance the terrestrial photosynthesis rate, *Atmos. Chem. Phys.*, *16*(3), 1479-1489, doi:10.5194/acp-16-1479-2016.

Zhang, J., and J. S. Reid (2010), A decadal regional and global trend analysis of the aerosol optical depth using a data-assimilation grade over-water MODIS and Level 2 MISR aerosol products, *Atmos. Chem. Phys.*, *10*(22), 10949-10963.

Zhu, Z., et al. (2016), Greening of the Earth and its drivers, *Nature Clim. Change*, *advance online publication*, doi:10.1038/nclimate3004.

Table 1. Results for AOD, diffuse PAR response

Location	Lat, Lon (deg)	AOD Trend (% y^{-1}) 2001-2013		Diffuse Radiation Trend Modeled[2]		Diffuse PAR Response, β_1 (μmol CO_2 / μmol photon)		GPP Trend Upscaled[2]	GPP Trend Modeled[2]	
		Satellite[1]	Modeled[2]	(W m^{-2} y^{-1})	(% y^{-1})	Published[1]	Modeled[2]	(gC m^{-2} y^{-1})	(gC m^{-2} y^{-1})	(% y^{-1})
Eastern United States		-3.0	-4.9	-0.26	-0.6	NA	0.008	-0.97	-1.05	-0.11
SEARCH Centreville	32.903, 272.750	-4.6	-4.5	-0.37	-0.8	NA	0.001	-1.49	-1.40	-0.13
Howland Reference	45.207, 291.275	-3.0	-2.8	-0.08	-0.2	0.005	0.016	-0.11	-0.69	-0.08
Morgan Monroe	39.323, 273.587	-4.9	-3.1	-0.32	-0.7	0.009	0.000	-1.81	-0.73	-0.07
UMBS	45.559, 275.287	0.2	-3.2	-0.09	-0.3	0.011	0.008	-0.13	0.05	0.01

[1]MISR
[2]This work
[3]*Cheng et al.*, 2015, average of measurements at SZA < 60 deg

Figure 1. SO_2 emissions from EPA CEMS data, scaled to include "stationary fuel combustion" and "industrial and other process" sources not monitored by CEMS (see text). (a) SO_2 emissions for 1995. (b) Difference in SO_2 emissions between 1995 and 2013. (c) Total U.S. SO_2 emissions for 1995-2013.

Figure 2. Annual trends in AOD from 2001–2013 for summer (JJA) from (a) MISR Level 3 at 555 nm; (b) CESM model at 550 nm. (c) AOD values for MISR and CESM, showing JJA average for the eastern U.S., as defined by the yellow outline in (a) and (b). Stipples in this figure indicate p values ≤ 0.05.

Figure 3. Annual trends from 1995-2013 for summer (JJA) for (a) modeled diffuse radiation (FSDSVI) from CESM; (b) modeled GPP trend from CESM in absolute units; (c) modeled GPP trend from CESM in % y^{-1}; (d) calculated GPP trend from flux tower upscaling in absolute units, using visible direct and visible diffuse radiation from CESM model, MODIS landcover, and relationships between GPP, visible direction, and visible diffuse reported by *Cheng et al.* (2015). Stipples in this figure indicate p values ≤ 0.05. (e) Correlation plot showing GPP trends from the CESM model and flux tower upscaling for 1995-2013. The slope (solid black line) is 1.2 ± 0.2 with $r^2 = 0.35$, and the one-to-one line (grey dotted line) is shown. In all panels, the open green circles show the flux tower sites from *Cheng et al.* (2015) used for the upscaling calculation, and the open yellow circle shows the Alabama SEARCH site.

Figure 4. CESM modeled trends for AOD, diffuse radiation (FSDSVI), and GPP, shown together with GPP determined from flux tower upscaling. ΔGPP is equal to GPP – GPP_{1995} for each time series. Panels show: a) spatially averaged trends for the eastern U.S. (as defined by the yellow outline in Fig. 2a); (b) the SEARCH site in Centreville, Alabama; (c) the UMBS site, in Michigan.

Figure 1

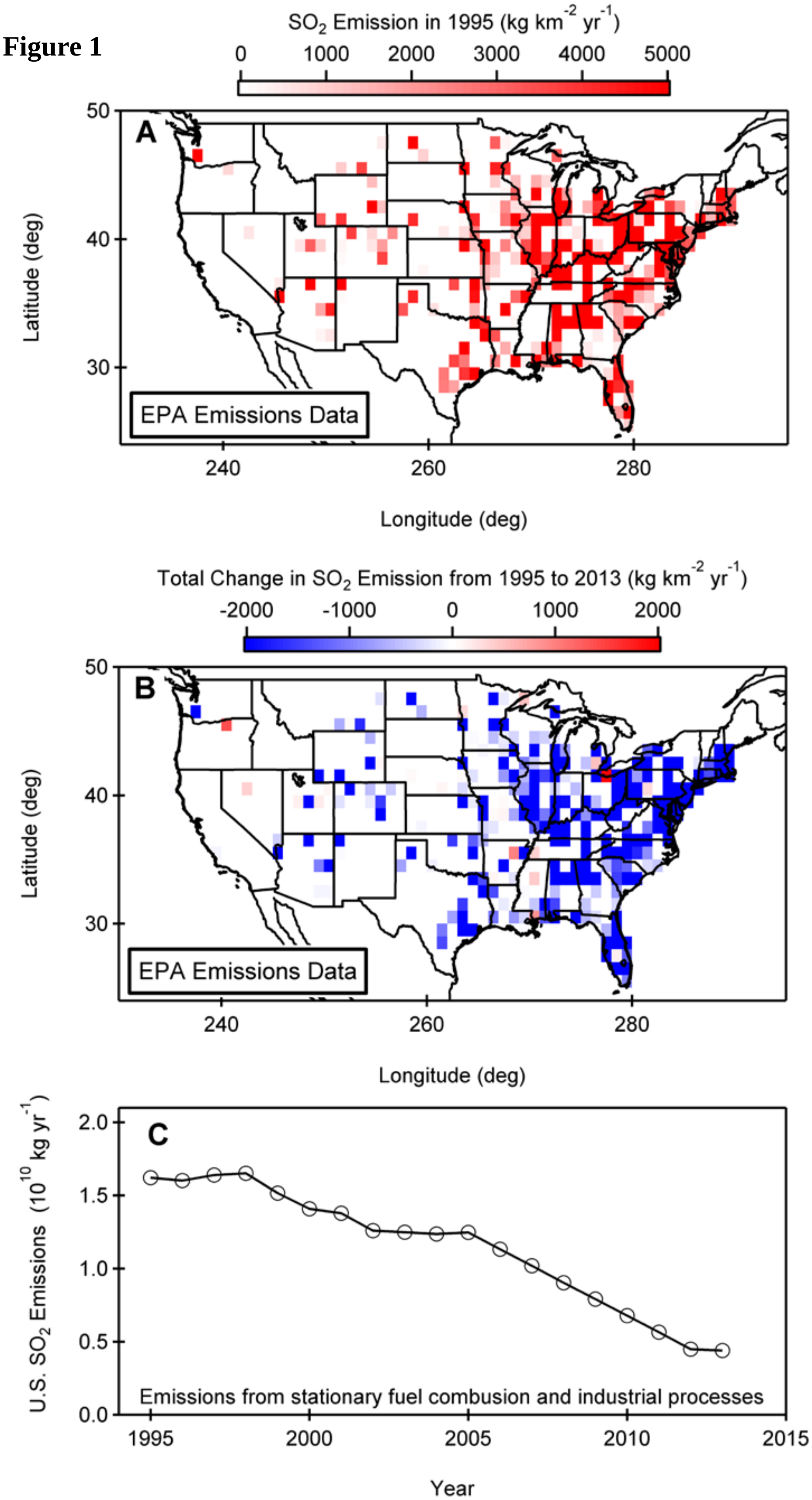
SO2 Emission in 1995 (kg km-2 yr-1)
0
1000
2000
3000
4000
5000
A
EPA Emissions Data
Latitude (deg)
50
40
30
240
260
280
Longitude (deg)
Total Change in SO2 Emission from 1995 to 2013 (kg km-2 yr-1)
-2000
-1000
0
1000
2000
B
EPA Emissions Data
Latitude (deg)
50
40
30
240
260
280
Longitude (deg)
C
U.S. SO2 Emissions (10^10 kg yr-1)
2.0
1.5
1.0
0.5
0.0
Emissions from stationary fuel combusion and industrial processes
1995
2000
2005
2010
2015
Year

Figure 2

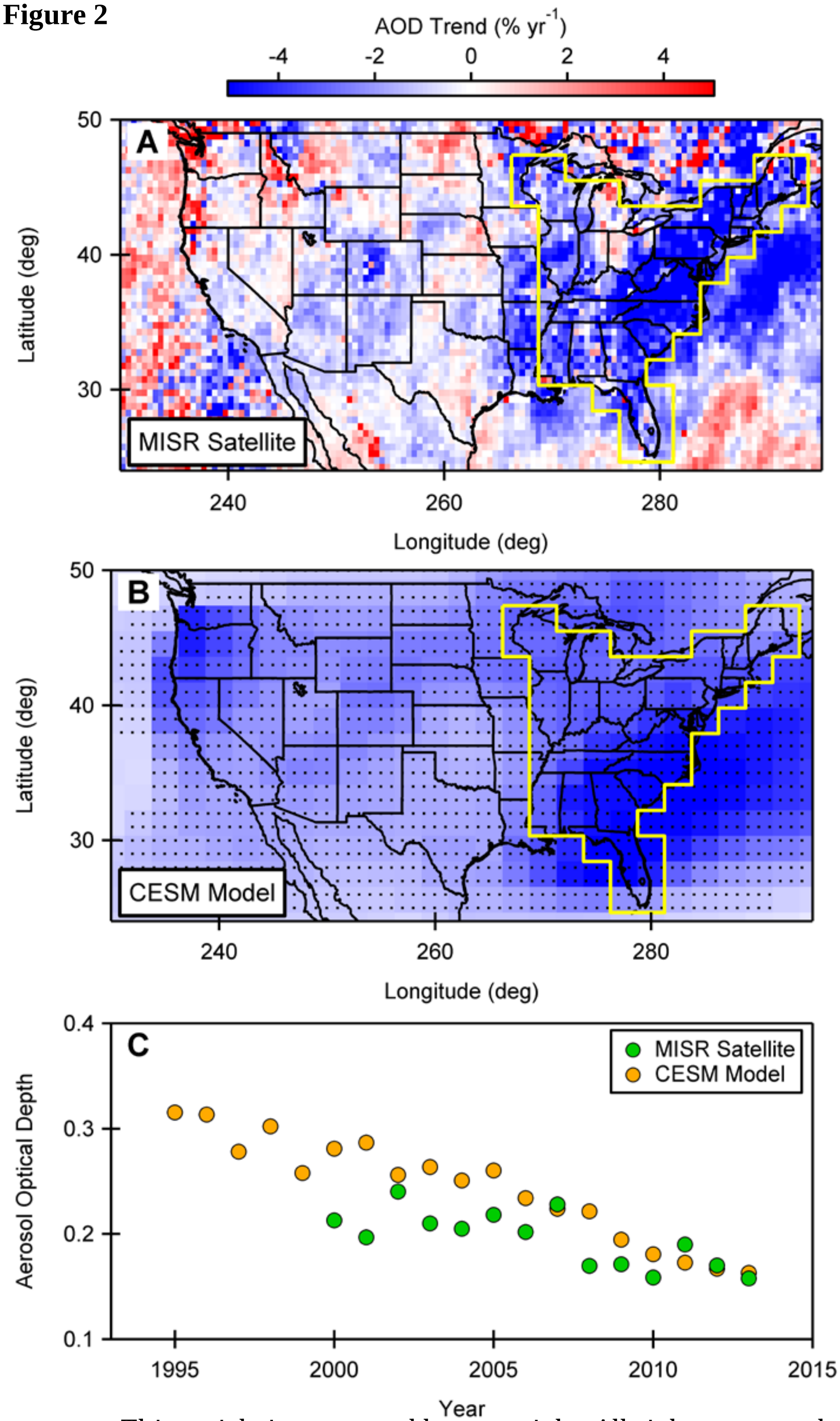
AOD Trend (% yr^{-1})
-4
-2
0
2
4
A
MISR Satellite
Latitude (deg)
Longitude (deg)
B
CESM Model
C
MISR Satellite
CESM Model
Aerosol Optical Depth
Year

Figure 3

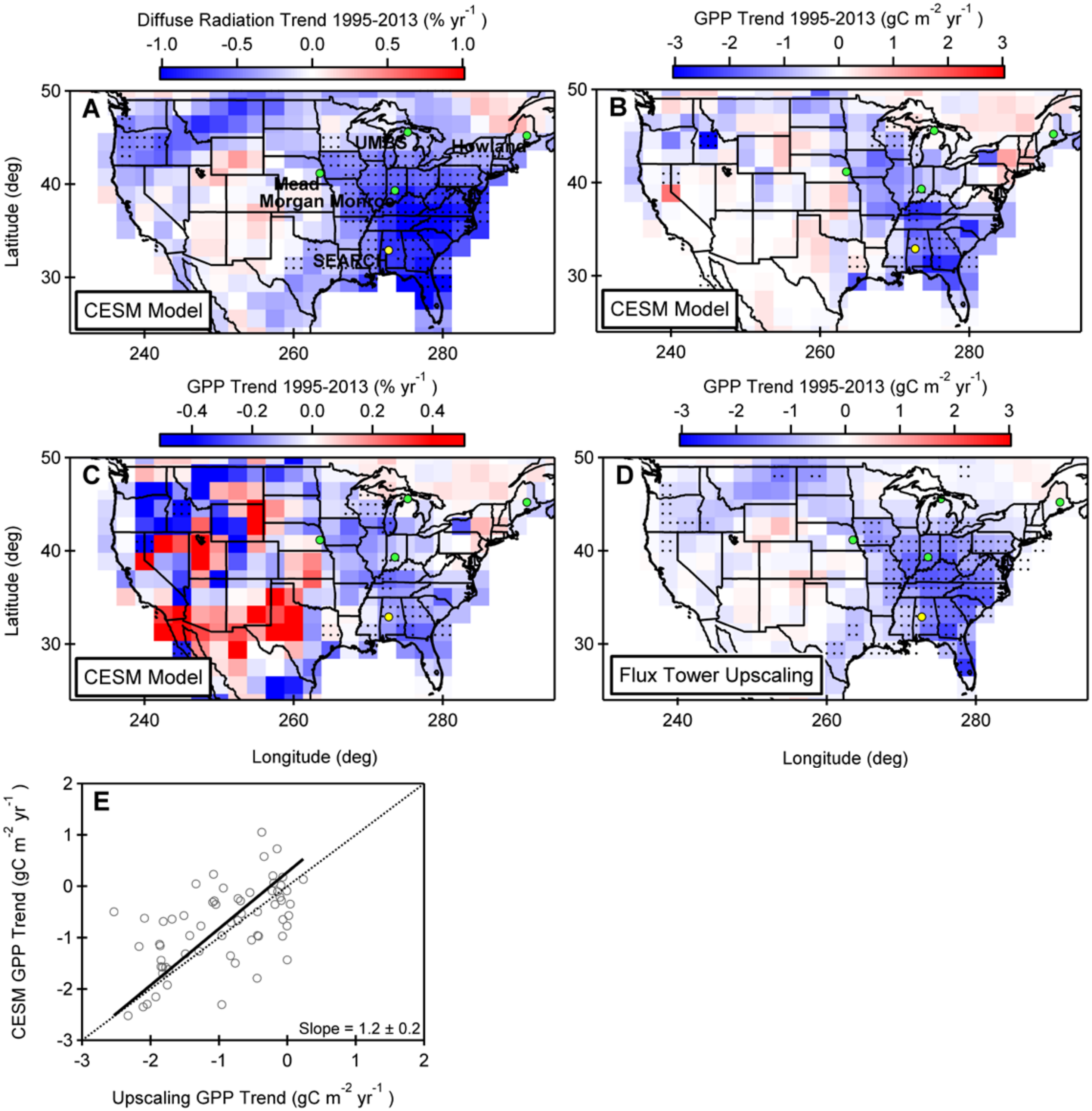
Diffuse Radiation Trend 1995-2013 (% yr-1)
-1.0 -0.5 0.0 0.5 1.0
A
UMBS
Howland
Mead
Morgan Monroe
SEARCH
CESM Model
B
GPP Trend 1995-2013 (gC m-2 yr-1)
-3 -2 -1 0 1 2 3
CESM Model
C
GPP Trend 1995-2013 (% yr-1)
-0.4 -0.2 0.0 0.2 0.4
CESM Model
D
GPP Trend 1995-2013 (gC m-2 yr-1)
Flux Tower Upscaling
Latitude (deg)
Longitude (deg)
50 40 30
240 260 280
E
Slope = 1.2 ± 0.2
CESM GPP Trend (gC m-2 yr-1)
Upscaling GPP Trend (gC m-2 yr-1)
2 1 0 -1 -2 -3

Figure 4

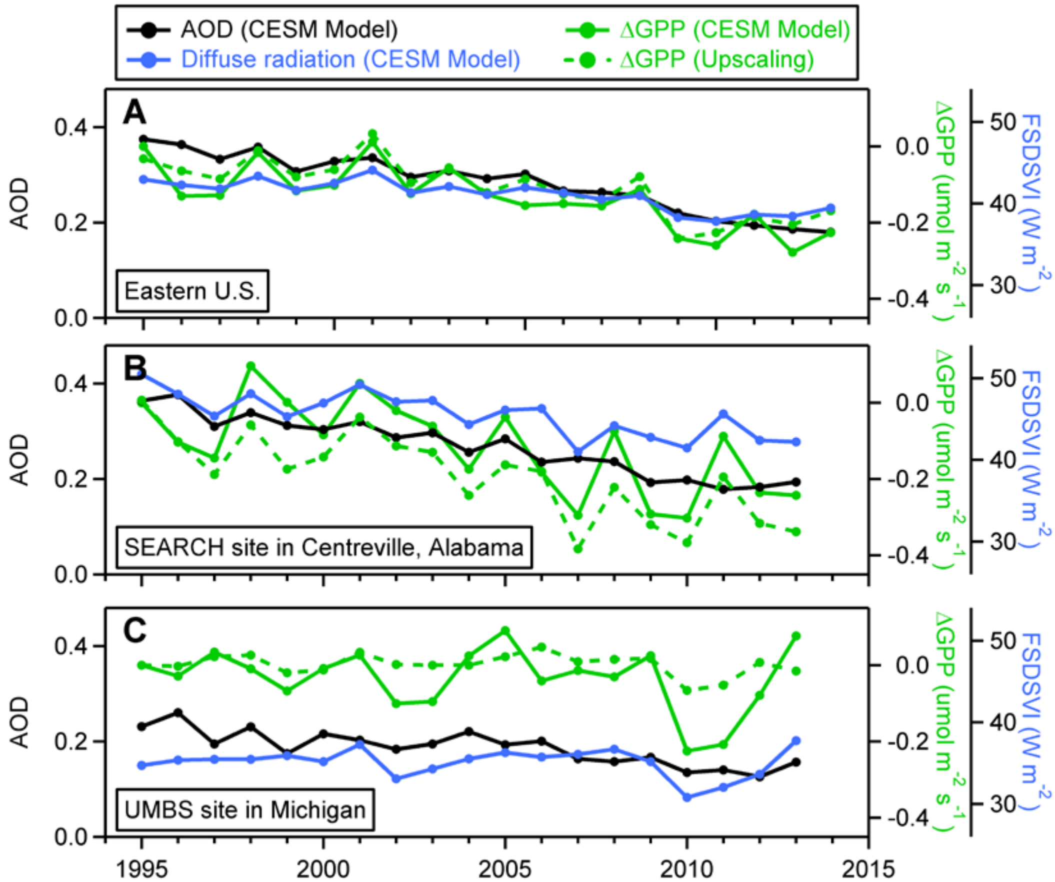
AOD (CESM Model)
Diffuse radiation (CESM Model)
ΔGPP (CESM Model)
ΔGPP (Upscaling)
A
Eastern U.S.
B
SEARCH site in Centreville, Alabama
C
UMBS site in Michigan
AOD
ΔGPP (umol m-2 s-1)
FSDSVI (W m-2)
0.0
0.2
0.4
-0.2
-0.4
30
40
50
1995
2000
2005
2010
2015

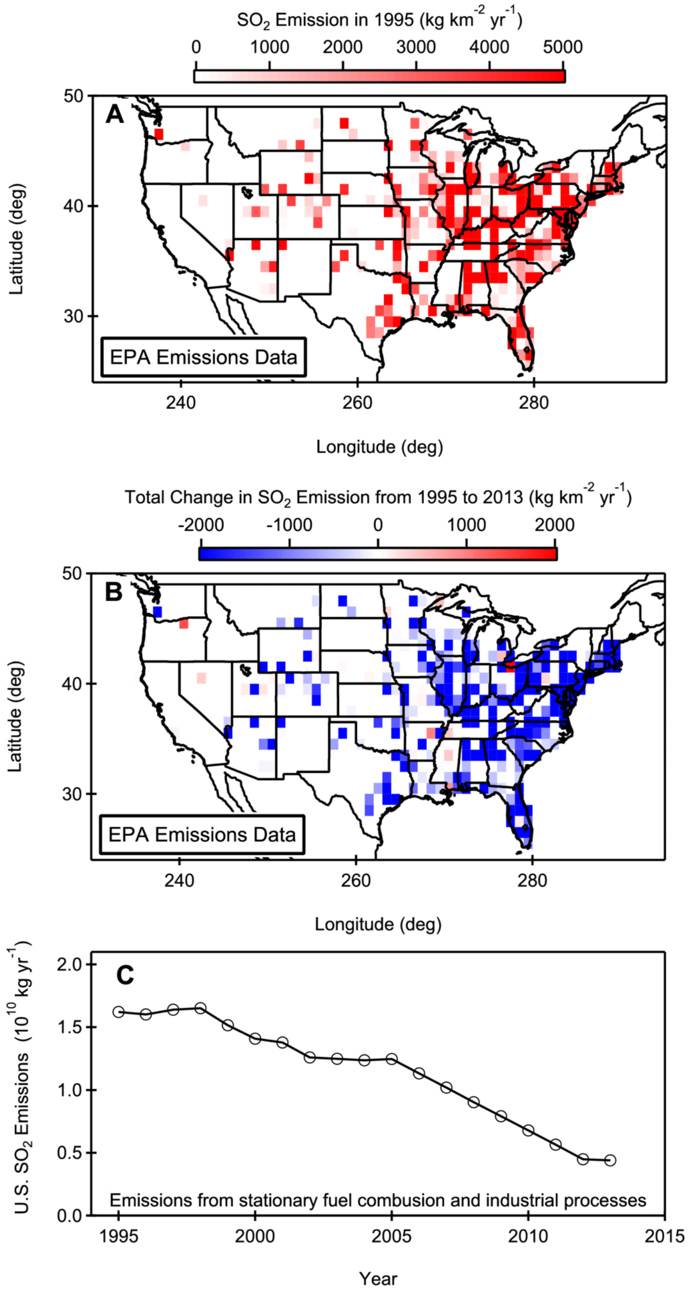

2016gl070052-f01-z-.eps

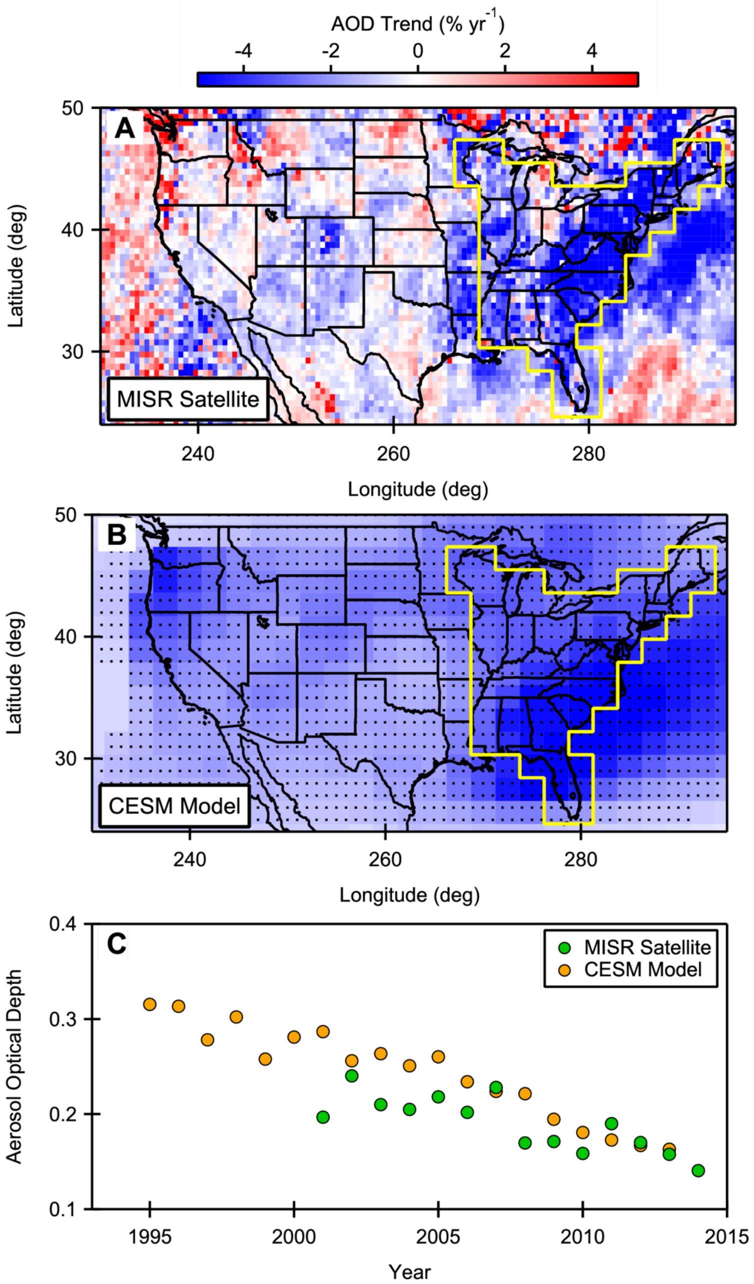

2016gl070052-f02-z-.eps

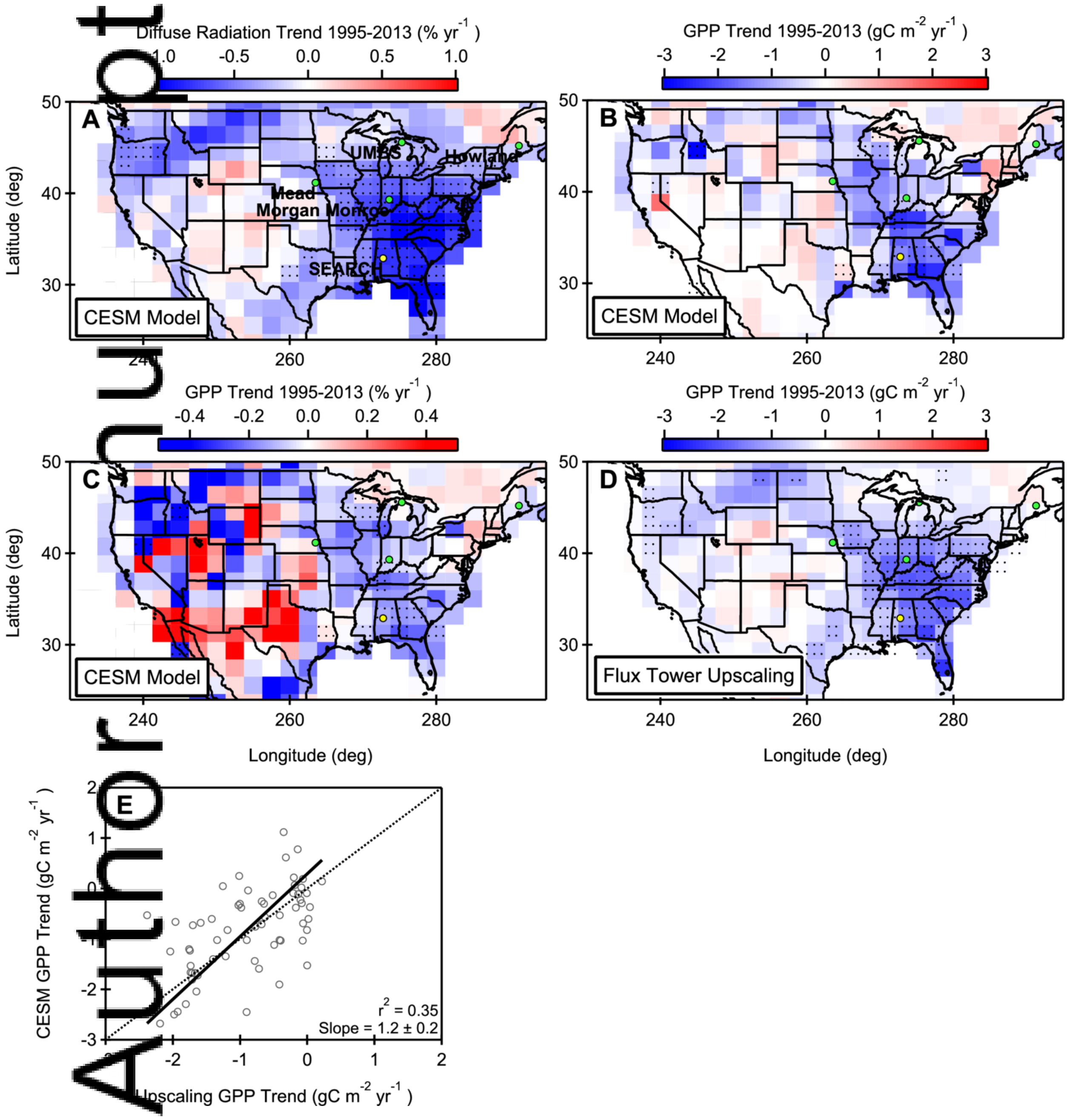

2016gl070052-f03-z-.eps

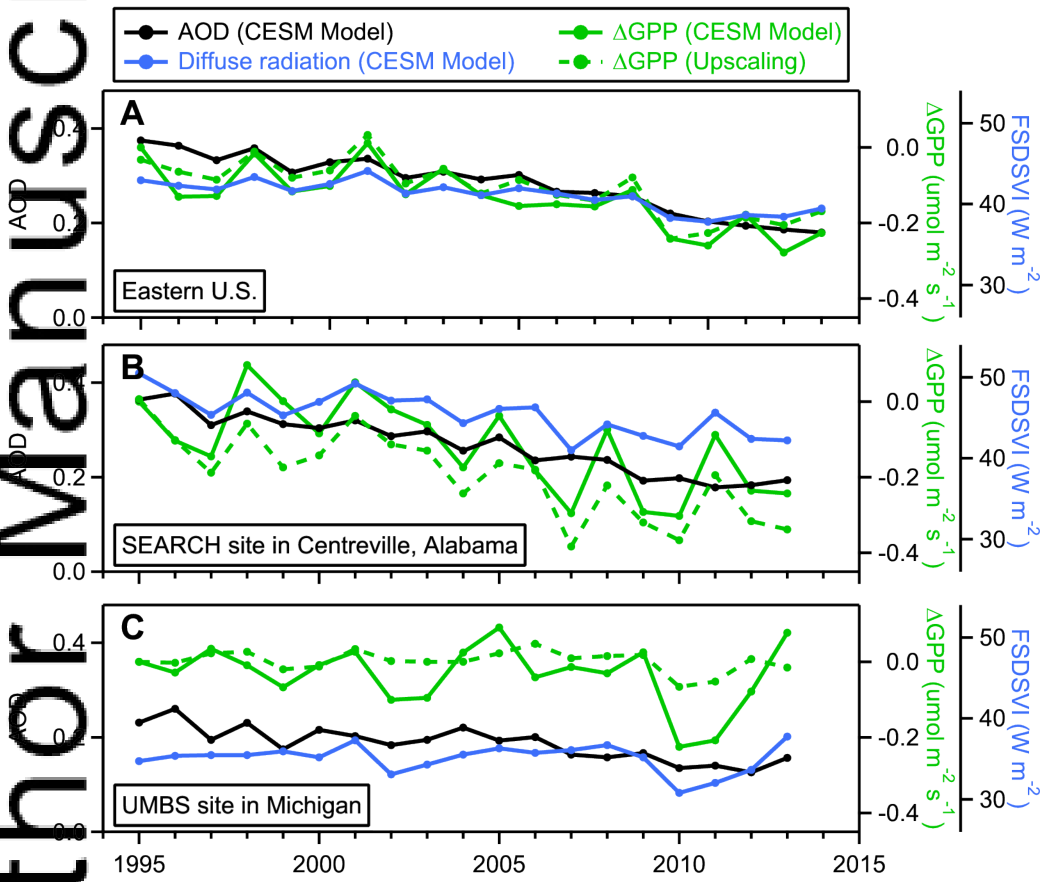

2016gl070052-f04-z-.eps